INTERNATIONAL ATOMIC ENERGY AGENCY
UNITED NATIONS EDUCATIONAL, SCIENTIFIC AND CULTURAL ORGANIZATION

INTERNATIONAL CENTRE FOR THEORETICAL PHYSICS
34100 TRIESTE (ITALY) - P.O.B. 586 - MIRAMARE - STRADA COSTIERA 11 - TELEPHONES: 224281/2/3/4/5/6
CABLE: CENTRATOM - TELEX 460392-1

SMR/110/A - 13

WORKING PARTY

ON

"PHYSICS OF CONDENSED MATTER AT PLANETARY PRESSURES"

(20 August - 7 September 1984)

SOLID STATE CREEP

(Part II)

B.K. ATKINSON

Geology Dept., Imperial College

London SW7 2BP, England

DEFECT CHEMISTRY AND CREEP

Defect concentration within neutrality range

$2[V_O^{\cdot\cdot}] \approx n$ for pure quartz

dominance of charged oxygen vacancies in controlling charge on crystal is balanced by free electrons.

Thus, for example

$$n(\text{free electrons}) = 2^{4/3} K_{Si}^{4/6} K_O^{4/3} K_{SiO_2}^{1/6} a_{SiO_2}^{1/6} a_{O_2}^{-1/6}$$

$$[V_O^{\cdot\cdot}] = 2^{-2/3} K_{Si}^{4/6} K_O^{4/3} K_{SiO_2}^{4/6} a_{SiO_2}^{4/6} a_{O_2}^{-1/6}$$

Can construct diagrams:-

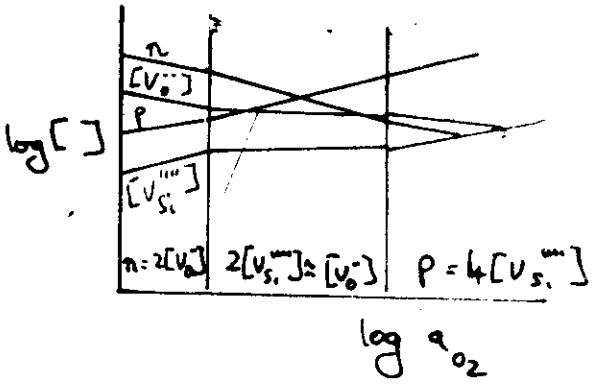

DEFECT CHEMISTRY AND CREEP

Realistic scale can be added to defect diagram for pure quartz

By following way in which a_{O_2} change effect properties believed to be dependent on defect concentration eg creep rates we can extricate which defects are important.

Pure quartz

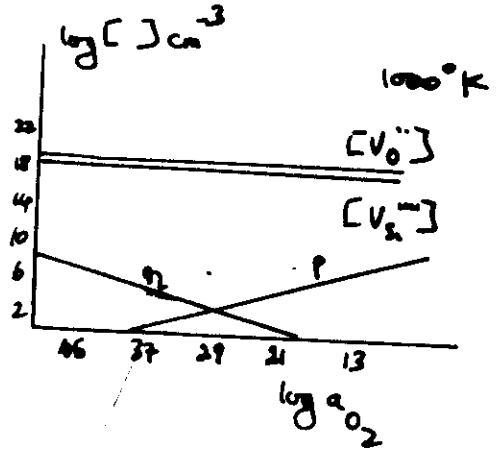

DEFECT CHEMISTRY AND CREEP

1. At low sulphur activities, creep controlled by neutral species, eg $(V'_{Pb} V_S^{\cdot})^{\times}$ whose concentration is independent of a_{S_2}.
2. At higher activities V'_{Pb} and $V_S^{\cdot}$ control creep rate.
3. Impurities, such as $B_i^{\cdot}$ or Ag act to increase or decrease $[\ ]$ of rate controlling defects and hence their influence can be gauged.

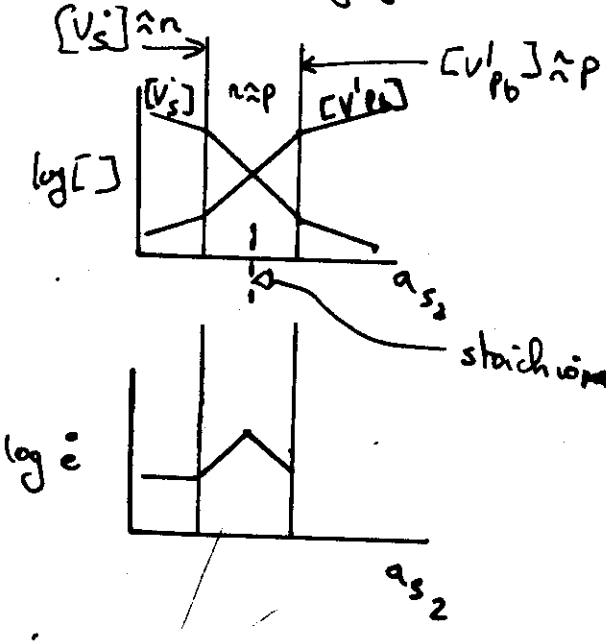

GENERAL CONCLUSIONS ON POINT DEFECTS

1. Under reducing conditions hydrogen incorporated interstitially in most silicates.
2. Under oxidizing conditions, main hydrogen defect seems to be 'hydrogarnet' defect.
   $(SiO_4)^{4-}$ replaced by $(H_3O_4)^{5-}$
3. Analysis of defect structure of 'dry' quartz where Al substitutes for silicon and is charge compensated by interstitial alkalis indicates a strong dependence of defect conc on f_{O_2}. Natural, impure, 'dry' quartz should thus have creep rate dependent on f_{O_2}.

   However, Rate at which dry quartz equilibrates with dry oxygen atmosphere is so slow that the influence of f_{O_2} changes would never be observed
4. Introduction of 'hydrogarnet' defect in large concentrations leads to strong dependence of defect conc. on f_{O_2} and f_{H_2O} but in opposite senses.

   The strong dependence on f_{H_2O} is enough to explain hydrolytic weakening effect but f_{O_2} is also worth considering in view of small changes in f_{H_2O} that can be expected in lab + in nature.

FORSTERITE OLIVINE

TABLE 3. Dependence of Charged Defect Concentrations Upon Activities of Chemical Components for $[(3H)^{\cdot}_{Si}] \neq [H_i^{\cdot}]$

Defect	a_{Mg}	f_{O_2}	f_{H_2O}
V''_{Mg}	-1	-¼	+½
O''_i	+1	+¼	-½
V''_{Si}	+2	+½	-1
$H_i^{\cdot\cdot\cdot\cdot}$	-2	-½	+1
$(V''_{Mg}\cdot V_O^{\cdot\cdot})^{\times}$	-1	-¼	+½
$(V''_{Mg}\cdot V_O^{\cdot\cdot})^{\cdot}$	-½	-¼	+¼
$(V''_{Mg}\cdot V_O^{\cdot\cdot})^{''}$	-½	+¼	-¼
$(3H)^{\cdot}_{Si}$	+½	-¼	+¼

TABLE 4. Dependence of Charged Defect Concentrations Upon Activities of Chemical Components for $[H_i^{\cdot}] = [Al'_{Si}]$ in Quartz

Defect	a_{Si}	f_{O_2}	f_{H_2O}
V''_O	+1	+¼	-½
$H_i^{\cdot}$	-1	-¼	+¼
V''_{Si}	-2	-½	+1
$H_i^{\cdot\cdot\cdot\cdot}$	+2	+½	-1
$(V''_{Si}\cdot V_O^{\cdot\cdot})^{\times}$	-½	-¼	+¼
$(V''_{Si}\cdot V_O^{\cdot\cdot})^{\cdot}$	-¼	+¼	-¼
$(V''_{Si}\cdot V_O^{\cdot\cdot})^{''}$	-¼	-¼	+¼
$(3H)^{\cdot}_{Si}$	-¼	+¼	+¼

TABLE 5. Defect Chemistry of Forsterite, Incorporating Hydrogen and the "Hydrogarnet" Defect

Reaction	Equilibrium Constant	Law of Mass Action
Incorporation of Hydrogen Interstitials		
$H_2 = 2H_i^{\cdot}$	K_H	$[H_i^{\cdot}]^2 = K_H f_{H_2}$
Ionization of Hydrogen Interstitials		
$H_i^{\cdot} = H_i^{\times} + e'$	$K_{H'}$	
Incorporation of the Hydrogarnet Defect		
$3H_2O = 2(3H)^{\cdot}_{Si} + 3H_O^{\times} + V''_{Si}$	K_{3H}	
Ionization of the Hydrogarnet Defect		
$(3H)^{\cdot}_{Si} = (3H)^{\times}_{Si} + h^{\cdot}$	$K_{3H'}$	$[(3H)^{\cdot}_{Si}] = K'_{3H} K_{3H'} K_H^{-\frac{3}{2}} f_{H_2}^{-\frac{1}{2}} f_{H_2O}^{\frac{3}{2}}$

TABLE 6. Defect Chemistry of Forsterite for the Reservoir Field $[(3H)^{\cdot}_{Si}] = 3[V''_{Si}]$

Defect	a_{Mg}	f_{O_2}	f_{H_2O}
V''_{Mg}	•	-1	•
O''_i	•	+1	•
V''_{Si}	•	+2	•
$H_i^{\cdot\cdot\cdot\cdot}$	•	-2	•
$(V''_{Mg}\cdot V_O^{\cdot\cdot})^{\times}$	•	-1	•
$(V''_{Mg}\cdot V_O^{\cdot\cdot})^{\cdot}$	•	-½	•
$(V''_{Mg}\cdot V_O^{\cdot\cdot})^{''}$	•	-½	•
$H_i^{\cdot}$	•	+½	•
$(3H)^{\cdot}_{Si}$	•	+½	•

TABLE 7. Defect Chemistry of Forsterite for the Reservoir Field $[H_i^{\cdot}] = [Al'_{Si}]$

Defect	a_{Mg}	f_{O_2}	f_{H_2O}
V''_{Mg}	•	+½	•
O''_i	•	-½	•
V''_{Si}	•	-1	•
$H_i^{\cdot\cdot\cdot\cdot}$	•	+1	•
$(V''_{Mg}\cdot V_O^{\cdot\cdot})^{\times}$	•	+½	•
$(V''_{Mg}\cdot V_O^{\cdot\cdot})^{\cdot}$	•	+¼	•
$(V''_{Mg}\cdot V_O^{\cdot\cdot})^{''}$	•	+¼	•
$H_i^{\cdot}$	•	-½	•
$(3H)^{\cdot}_{Si}$	•	-½	•

Albite Feldspar

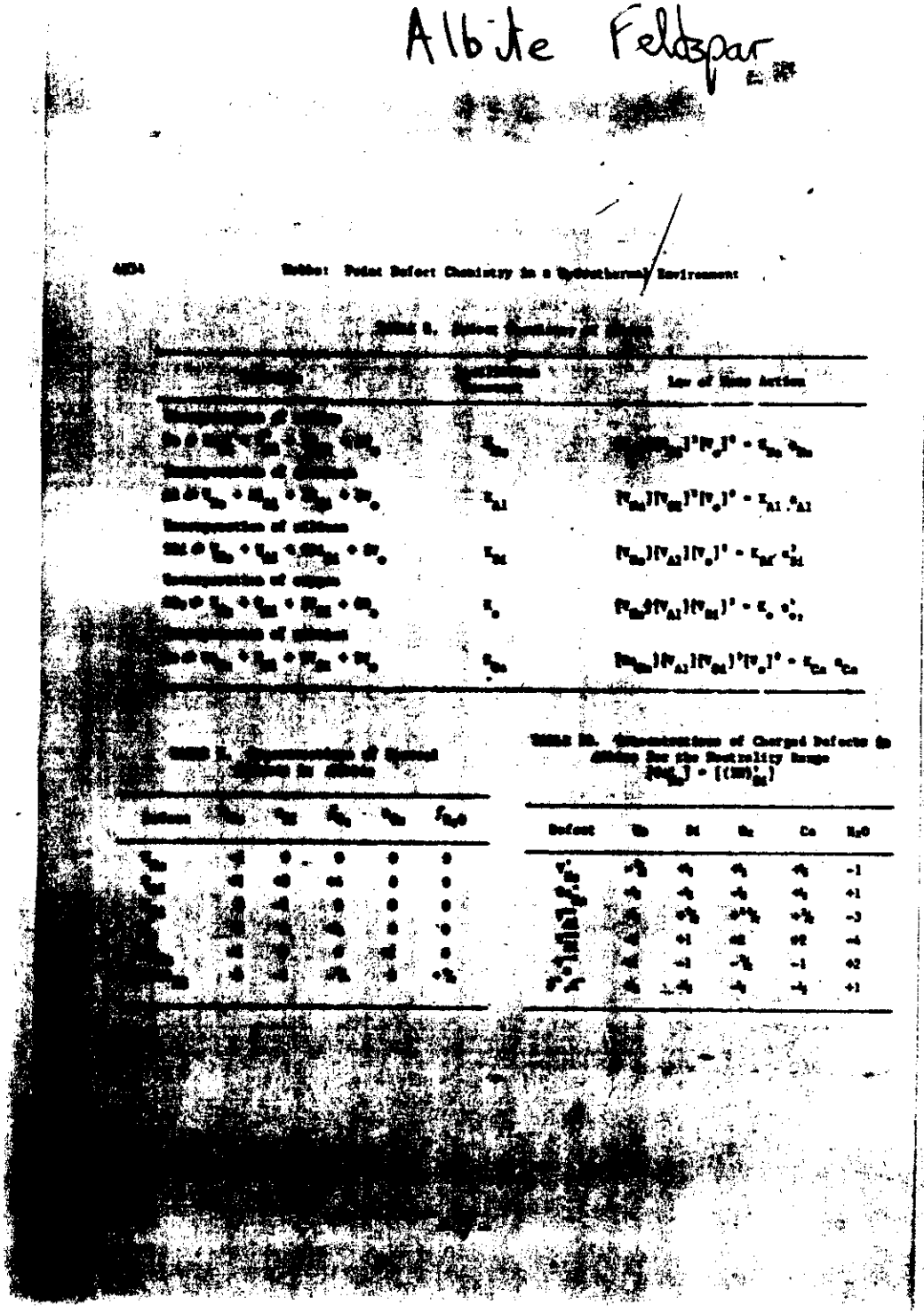

DIFFUSION DATA FOR QUARTZ

(Dennis)

1. Water fugacity dependence at 700°C

$$D_{ox} \propto f(H_2O)^m$$

$m = -0.11 \pm 0.29$ (∥c)
$m = 0.01 \pm 0.51$ (⊥c)

i.e. essentially independent over $f(H_2O)$ 11-77 MPa

2. (Giletti/Yund)

$$D_{ox} \propto f(H_2O)^{1.1}$$

a marked dependence over $f(H_2O) = 22.5 - 225$ MPa

3. Why differences?

PROBLEMS: Both studies used restricted $f(H_2O)$ range and errors quite large (age). Thus within experimental error, both studies are compatible.

At high total pressure (350 MPa) used by Giletti/Yund quartz shows significant solubility in water. Possible influence of solution effects on diffusion profile must be considered.

TABLE 4. Summary of Oxygen Tracer Diffusion in Quartz

Study[a]	Method[b]	T°C	Orientation	D_0, $m^2 s^{-1}$	ΔH, kJ mol^{-1}	Conditions[c]	Reference
[illegible]	SIMS	700-850	∥ c	2.1 × 10^{-11}	[illegible]	HMO	this study
[illegible]	SIMS	700-800	⊥(10$\bar{1}$0)	3.9 × 10^{-10}	[illegible]	[illegible]	this study
[illegible]	SIMS	600-[illegible]	∥ c	3.0 × 10^{-11}	[illegible]	H_2O	Giletti and Yund [this issue]
[illegible]	SIMS	600-[illegible]	⊥(10$\bar{1}$0)	2.3 × 10^{-11}	[illegible]	H_2O	Giletti and Yund [this issue]
[illegible]	SIMS	500-550	∥ c	3.5 × 10^{-1}	272.1	H_2O	Giletti and Yund [this issue]
[illegible]	SIMS	600-750	∥ c	1.1 × 10^{-15}	133	HMO	Freer and Dennis [1982]
[illegible]	BA	667	∥ c	D_{667} = 4.1 × 10^{-16} $m^2 s^{-1}$		e	Choudhury et al. [1965]
[illegible]	BA	667	⊥(10$\bar{1}$0)	D_{667} = 6.1 × 10^{-18} $m^2 s^{-1}$		e	Choudhury et al. [1965]
[illegible]	BE	1010-1212	Isotropic	3.7 × 10^{-13}	130.23	1 × 10^4 Pa[d]	Haul and Dümbgen [1962]
[illegible]	BE	870-1180	Isotropic	1.1 × 10^{-14}	195	2 × 10^4 Pa[d]	Schachtner and Sockel [1977]

[illegible] Buffer not known, 82 MPa P(H_2O).

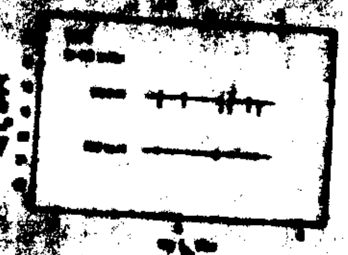

[illegible]

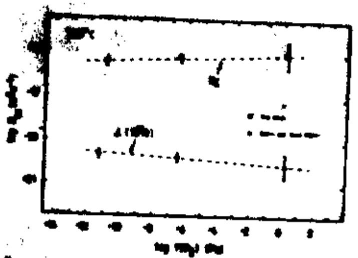

Fig. 5. Measured values of log D_{Ox} as a function of log $f(O_2)$ at 700°C. The closed symbols represent data from this study (Table 3) and the open symbols are data taken from Giletti and Yund [this issue]. The $f(O_2)$ for the latter results was calculated from the equilibrium constant for formation of water at 700°C [Robie et al., 1978] and the total pressure, P = 100 MPa. The slopes for both orientations clearly indicate $f(O_2)$-independent behavior for tracer diffusion.

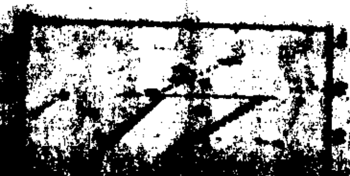

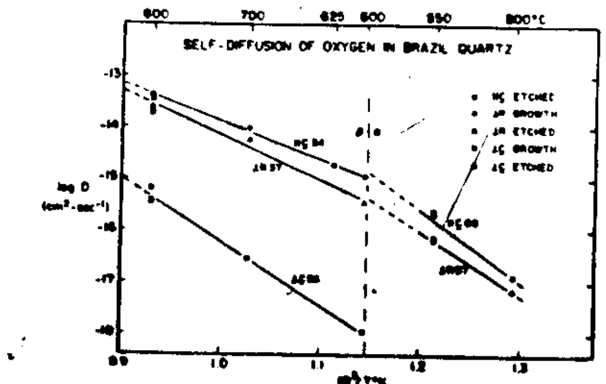

Fig. 3. Arrhenius plot of self-diffusion coefficient D for natural quartz crystal versus 1/T°K at 100-MPa water pressure. Each point represents the average of all measurements made for that temperature, crystallographic direction, and surface condition. The α-β transition temperature at 100 MPa is shown by the vertical dashed line. Solid lines are least squares fits of data in α or β field. Numbers next to lines are activation energies in kilocalories per mole. The dotted line shows a least squares calculation (transport parallel to c) combining the data from the α and β fields. It should be compared with the two topmost solid lines, which show the best fit to the data.

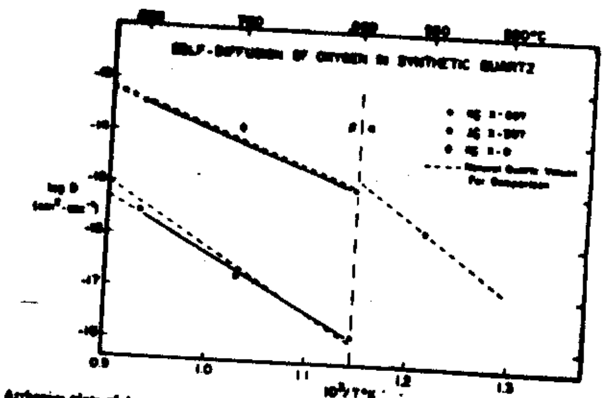

Fig. 4. Arrhenius plots of data as in Figure 3, but for synthetic crystals X-307 and X-0. Solid lines are fitted to the data, while dashed lines are from the natural quartz data shown in Figure 3.

Griffin and Yu

TABLE 4 Preexponential Factor (D_0) and Activation Energy for Arrhenius Relation

Parameter	α Quartz, 500–550 °C	β Quartz, 600–800 °C	e-of-c
Diffusion Parallel to c Axis, Brazil Crystal			
D_0, cm²/s	190	4.3×10^{-1}	$1.2 \times$
Q, kJ/mol	284 ± 92	142 ± 4	171 ±
Q, kcal mol	68 ± 22	34 ± 1	41 ±
Diffusion Normal to Rhombohedron Face, Brazil Crystal			
D_0, cm²/s	9.59×10^{-1}	9.5×10^{-1}	$2.1 \times$
Q, kJ/mol	238 ± 12	155 ± 8	184 ±
Q, kcal mol	57 ± 3	37 ± 2	44 ±
Diffusion Normal to c Axis, Brazil Quartz			
D_0, cm²/s		1.1×10^{-4}	
Q, kJ/mol		234 ± 8	
Q, kcal mol		56 ± 2	
Diffusion Normal to c Axis, Synthetic Crystal X-107			
D_0, cm²/s		2.2×10^{-4}	
Q, kJ mol		205 ± 12	
Q, kcal mol		49 ± 3	

See text for discussion of how uncertainties were calculated

Fig. 6. Comparison of published diffusion data for hydrogen and oxygen. Key to reference numbers next to curves. 1, this work; 2, Hetherington and Jones [1962], dry experiments; 3, Chaudhuri et al. [1965], at 820 bar water pressure; 4, Shaffer et al. [1974], hydrogen; 5, Kats et al. [1962], hydrogen; and 6, Giletti et al. [1978], oxygen diffusion in albite and orthoclase feldspars.

Fig. 5. Effect of water pressure on diffusion in quartz. Plotted as log diffusion coefficient (D) versus log water fugacity. Shows two data ranges of observed values. Triangle is data for synthetic quartz X-107; circles are for natural quartz. All for measurements parallel to c with. Numbers on lines are slope values.

DEFECT CHEMISTRY AND DIFFUSION MECHANISMS

After Dennis data.

1. Independence of D_{ox} with $f(H_2O)$ and $f(O_2)$ is not consistent with dissolved structural water in the lattice limiting oxygen transport.

2. All models of water incorporation in quartz and influence on diffusion of oxygen predict

$$D_{ox} \propto f(H_2O)^m$$

where m is $>+0.5$ or <-0.5

3. Results are consistent with material whose point defect structure is controlled by either
(a) thermal ionic disorder, or
(b) non-volatile, aliovalent impurity
(c) transport system must involve a charged defect

4. Most probable thermal defect is Schottky one with conc. of 10^{-3} mol % at 1000°K. But defect conc. in Dennis work are at least 10^{-2} mol %, so some sort of impurity disorder is likely to be dominant.

5. Due to high conc. of Al (2.5×10^{18} Al cm^{-3}) in test specimens – data accounted for by Main defects are: divalent vacancies of oxygen, created for incorporation of Al atoms into Si sites.

RUTTER/RAWLINGS MODEL

FOR LOW STRESSES

$$\dot{e} = 32\, w D_b C_0 \sigma / \rho R T d^3$$

w = grain boundary film width
D_b = thin film diffusion coefficient
C_0 = solubility of mobile phase in unstressed sink solution (depends on pore pressure and temperature)
σ = applied stress difference
ρ = density of solid, R = gas constant, T = °K
d = grain size

FOR A SINUSOIDAL GRAIN BOUNDARY

$$\dot{u} = (8\tau C_0(p,T)\, w D_b / h^2 \rho)(\partial \ln C_0 / \partial p)_T$$

$\dot{u}$ — sliding rate; τ — shear stress; h — amplitude of g.b. asperities

$$\dot{e} = K \dot{u} / d$$

$\dot{e}$ — in fault zone; d — grain size in fault zone; K — fraction of grain sliding

PROBLEMS WITH RUTTER/RAWLINGS MODEL

Major uncertainties lie in choice of w, C_0, D_b
(w — film width; C_0 — solubility; D_b — diffusion coefficient)

N — assumed constant + uniform at low stress
But must be squeezed out of region of compression precisely where it is most needed.
Even if polar layers of high viscosity in fluid maintain a layer with finite thickness the linear dependence of strain rate on stress is likely to be lost.

w assumed $\simeq 10^{-9}$ m

If high viscosity in reason fluid remains between grains then it must have different properties to bulk fluid

D_b — Bounded initially by diffusivities in aqueous sol^{n}s ($10^{-8} - 10^{-9}$ m^2.s^{-1})
and in common minerals — ($\ll 10^{-20}$ m^2.s^{-1} at low T/T_m)

② Estimate from Stokes/Einstein/Sutherland relation
But include retardation factor (10^{-5}) because of thin film effects

$$D = kT / m\pi\eta(a/2) \qquad 4 \leq m \leq 6$$

D — diff. coeff. of solute particle in bulk fluid; η — shear viscosity of solvent; $a/2$ — solute particle diameter

(2) They used incorrect expression for Stokes/Einstein. Corrected given $D_b = 2 \times 10^{-14}\ m^2 s^{-1}$ (300°C, P_{H_2O} = 200 bar)

(3) Viscosity of thin film must be of same order as solid or stressed fluid would be continually expelled from intergrain region.

$$\eta_e = (\Delta\sigma / 3\dot{\varepsilon})$$

η_e: equivalent viscosity for flow of rock; $\Delta\sigma$: stress difference; $\dot{\varepsilon}$: strain rate

$$D_b = 10^{-19} \rightarrow 10^{-24}\ m^2 s^{-1}$$

(4) Experiment (Brady) – estimated maximum D_b for silica through tight grain boundaries in presence of aqueous fluid.

$$D_b = 7 \times 10^{-15}\ m^2 s^{-1}$$

CONCLUDE: Question validity of Stokes/Einstein to thin situation

Because of uncertainty in parameters not fruitful at present to compare experiment with Rutter/Mainprice theory.

1. Liquid has some solubility for solid.
2. Liquid penetrates boundary between grains by cracking rock between particles.
3. Stressed cracked rock rests so that plastic flow or creep becomes likely.
4. Aggregate deforms and rock grows again.

$$\dot{\gamma} = 3/2\ \dot{e}_o \left(\sigma_1^2 - \sigma_1\sigma_2 + \sigma_2^2/\sigma_y^2\right)(\sigma_1 - \sigma_2 / \sigma_1 + \sigma_2)$$

$\dot{\gamma}$: shear strain rate

σ_1, σ_2: principal stresses at failure

σ_y = yield stress

$$\dot{e}_o = 8 D_L C_L \Gamma \Omega / \pi k T r^3$$

D_L = diffusivity of solid in liquid

C_L = solubility of solid in liquid

Γ = surface energy of solid/liquid interface

Ω = atomic/molecular volume of diffusing species

k = Boltzmann's constant

$2r = d$ = grain size

Incorporate third power stress dependence of strain rate as yield stress is not a constant but is found experimentally to have this dependence in hydrolytically weakened state.

NON-EQUILIBRIUM THERMODYNAMICS OF PRESSURE SOLUTION

Lehner / Bataille 1984

1. Essential feature of Rutter (and others) p. sol^n theories is that there exists an adsorbed intergranular film of fluid that transmits the full intergranular normal stress and supports shear stresses.
(Follows earlier work by Weyl).

2. These models use Gibbs fundamental equilibrium condition for a stressed solid in contact with its aqueous solution.
Local chemical potential of solid component in the solution film is then LINEARLY related to the local intergranular normal stress.
Rapid creep in presence of fluid is explained by exponentially stress enhanced solubility along grain to grain contacts, providing driving force for diffusive mass transfer.

PROBLEM: Use of Gibbs' equilibrium condition cannot be reconciled with existence of large shear stresses in the film, which are needed to maintain mechanical equilibrium if the film is to maintain the total grain to grain contact force.

NEED TO REPLACE GIBBS CONDITION WITH EQUILIBRIUM CONDITION FOR FIRST ORDER TRANSITION OF PHASE UNDER NON HYDROSTATIC STRESS (A EASY SOLUTION)

-17-

PATERSON'S "INERT LOADING FRAME"

Useful notion of inert loading frame

1. Fluid-permeated
2. Capable of transmitting arbitary tractions across grain boundary
3. Permits contact between hydrostatically stressed grain boundary fluid and a dissolving solid.
4. Can be given clear physical interpretation of a fluid permeated contact zone at grain to grain contact strain rate fluid permeated gouge layer fault

PROBLEM: Paterson's generalization of Gibbs equilibrium condition does not hold true when loading frame given interpretation 4 above

It is only valid as an approximation when interpretation 4 above replaced with adsorbed solution film supporting full contact stresses.

PROBLEM: Widely held that pressure solution rates of creep are diffusion controlled.
However, examination of silica-water reaction kinetics shows that below 300 °C solution/precipitation processes are interface reaction controlled.

LEHNER / BATAILLE

Pressure solution sliding

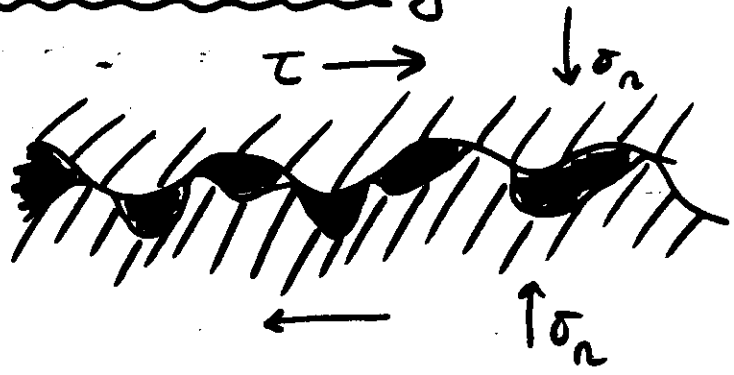

Solid portion of boundary 'strong'

For pressure solution creep, strain rates must be slow enough so that fast fracture does not occur and dry friction results for all asperity sizes.

Temps. must be low enough so that creep in solid does not occur in PARALLEL to pressure solution to relax loads on asperities

Then pressure solution creep viewed as operating in SERIES with process responsible for final crushing of asperities e.g. fast fracture - but also [redacted] stress corrosion

Rate of sliding then controlled by slowest of
1. Mechanical failure of asperities 2. Interface mass transfer 3. Solute diffusion

LEHNER / BATAILLE

For diffusion-controlled slip of gouge layer containing tensely packed particles (spherical)

$$\dot{\gamma} = \frac{120\,\bar{V}_p^s\, C_p \rho^f D \tau}{\rho^s R T \bar{\delta} r}$$

where $\dot{\gamma} = \dot{u}/h$ = shear rate, $\dot{u}$ = slip rate, h = boundary width (or gouge layer thickness)

$\bar{V}_p^s$ = molar volume of solid under hydrostatic stress
C_p = equilibrium solute concentration at precipitation site
ρ^f = fluid density
ρ^s = solid density
D = diffusion rate of species in solution
τ = shear stress
$\bar{\delta}$ = mean diffusion path length
r = ($1/r$ = specific surface area of particles - approximate to $\frac{1}{r_i}$ where r_i is the mean particle radius)

For interface reaction controlled slip

$$\dot{\gamma} = \frac{60\, k\, \bar{V}_p^s\, \rho^f \tau}{\rho^s R T r}$$

where
k = transfer coefficient

If $k\delta/2C_pD \ll 1$ process will be interface reaction controlled.

LEHNER / BATAILLE

Comparing shear strain rates for interface reaction control $\dot{\gamma}_I$ and diffusion control $\dot{\gamma}_D$

$$\dot{\gamma}_I / \dot{\gamma}_D = k\bar{S} / 2 C_p D$$

$\dot{\gamma}_I \approx 10^{-16} \tau / r$ from quartz/water data

If $r = 10^{-4}$ m (granite)
and
$\tau = 10^7$ Pa (100 bars)
then

$$\dot{\gamma}_I = 10^{-7}\ s^{-1}$$

This is about the experimentally determined point at which pressure solution weakening is observed.

CONCLUSIONS:

Pressure solution slip rates should, in general, depend on an effective normal stress. However, this effect may be negligible in many cases.

Interface reaction controlled slip rates are expected to be independent of pore fluid pressure.
Sometimes accords with experiment - sometimes does not.

CALCITE

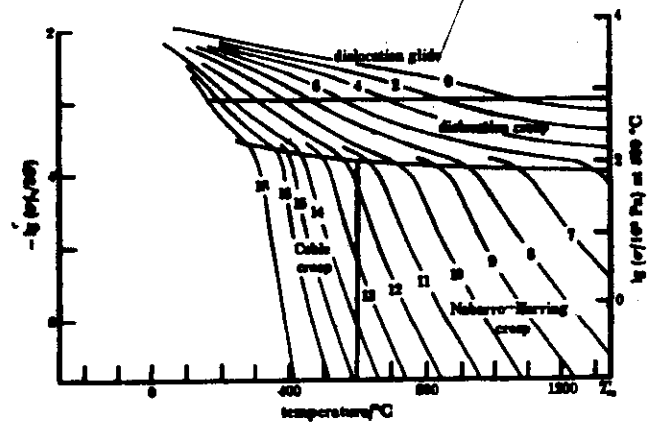

FIGURE 6. Deformation mechanism map for calcite without pressure solution. Contours of −lg strain rate are shown. σ is differential stress ($\sigma_1 - \sigma_3$). d = 100 μm; F = 37 cm³.

QUARTZ

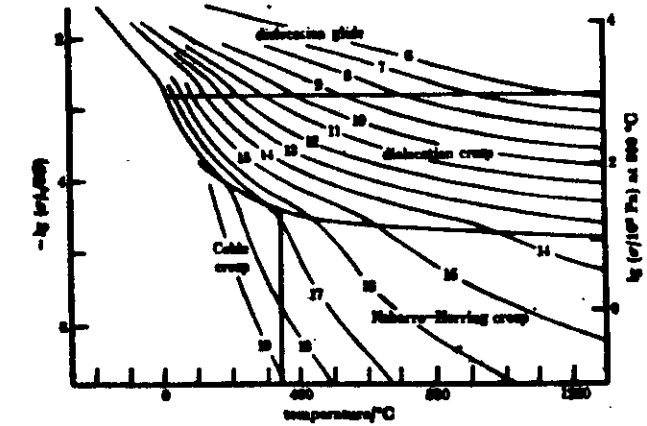

FIGURE 7. Deformation mechanism map for quartz without pressure solution. Contours of −lg strain rate are shown. σ is differential stress ($\sigma_1 - \sigma_3$). d = 100 μm; F = 30 cm³.

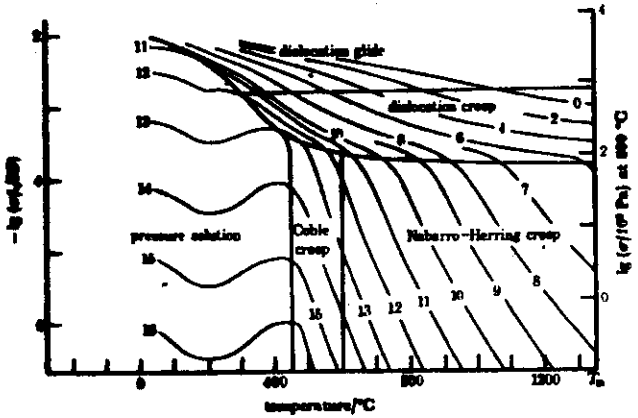

Figure 6. Deformation mechanism map for calcite modified by the addition of a pressure solution field. d = 100 μm; V = 37 cm³.

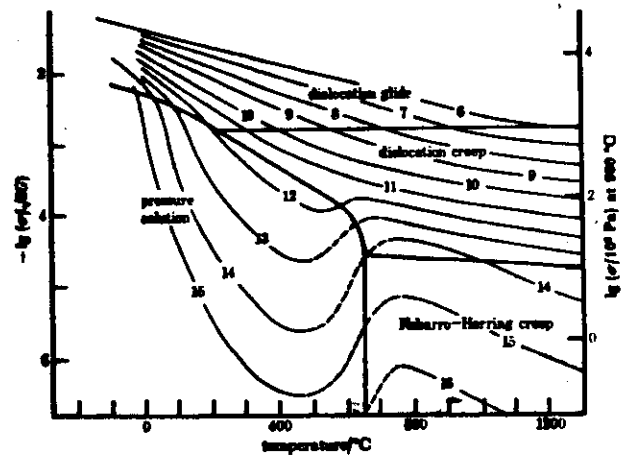

Figure 8. Deformation mechanism map for quartz modified by the addition of a pressure solution field. The region of dashed strain rate contours represents the inhibition of pressure solution through decrease in pore water concentration. d = 100 μm; V = 22 cm³.

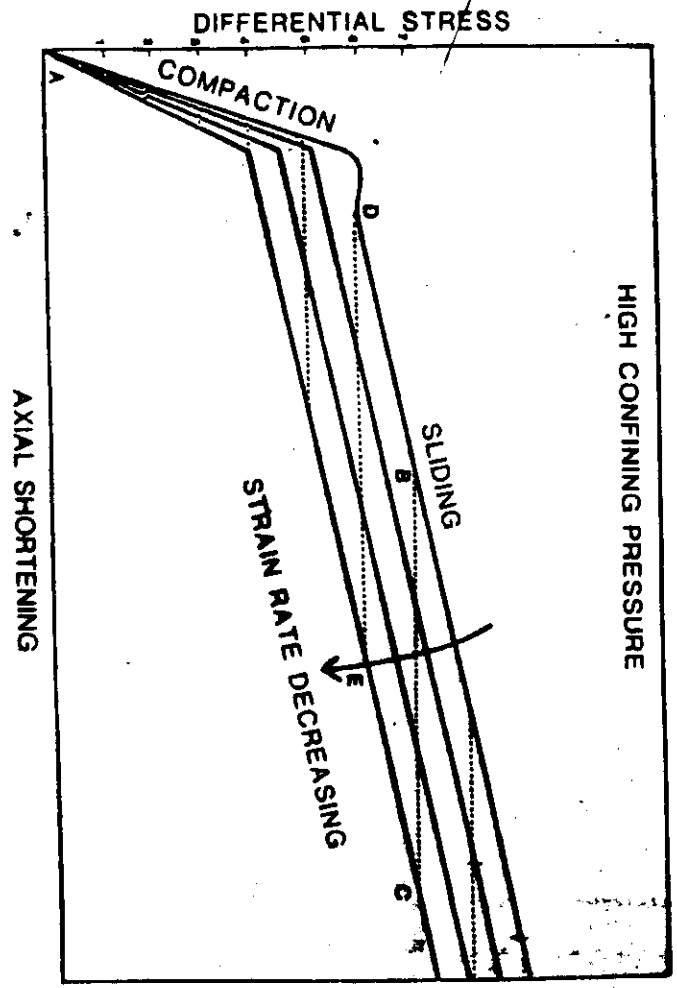

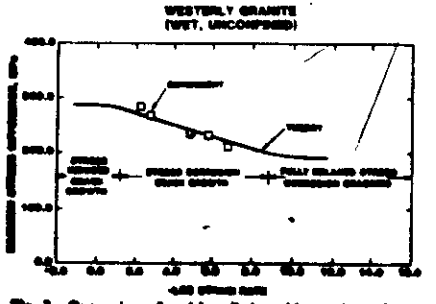

Fig. 7. Comparison of model predictions with experimental results for uniaxial failure strength of Westerly granite over a range of strain rates.

SUBCRITICAL CRACKING OF ROCKS

EXTRAPOLATION TO EARTH'S CRUST

1. $v = A_1 (K_I / K_{Ic})^{n_1}$ Charles

2. $v = A_2 \exp [n_2 (K_I / K_{Ic})]$ Wiederhorn-Bolz

3. $v = A_3 \exp [n_3 (K_I / K_{Ic})^2]$ Lawn

MECHANISMS OF SUBCRITICAL CRACKING IN ROCKS/MINERALS

1. STRESS CORROSION

(a) Quartz (and other silicates?)

$$XA + B \leftrightarrow B^* \rightarrow \text{PRODUCTS}$$

X = N° of environmental species A; B = single crack tip bond; B^* = activated state

e.g. $H\text{-}O\text{-}H + \left[\equiv Si\text{-}O\text{-}Si \equiv\right] \leftrightarrow \equiv Si\text{-}OH \cdot HO\text{-}Si \equiv$

$$\downarrow$$

$$2[\equiv Si\text{-}OH]$$

(b) More complex minerals (biotite, hornblende) may have constant volume complex chemical reaction catalyzed by stress intensity concentration

2. DIFFUSION

e.g. boundary, surface volume, vapour

3. DISSOLUTION

Concentrated at crack tip by stress assisted removal of dissolution products.

4. ION-EXCHANGE

+ local chemical changes in minerals involving volume changes

5. MICROPLASTICITY

inhomogeneous plastic deformation leading to stress concentrations, crack nucleation and growth by coalescence of microcracks

Table 1. Tensile crack growth rates in quartzite controlled by [redacted] boundary diffusion.

Grain size (micrometres)	Temperature (°C)	K_I (MPa.m$^{1/2}$)	Crack velocity (m.s^{-1})
10	200	1	7×10^{-13}
10	200	0.5	5.5×10^{-14}
10	400	1	2.2×10^{-10}
10	400	0.5	2.2×10^{-11}
1000	200	1	7×10^{-15}
1000	200	0.5	5.5×10^{-16}
1000	400	1	2.2×10^{-12}
1000	400	0.5	2.2×10^{-13}

$$\frac{da}{dt} = \frac{\Omega D_b \delta}{4 l^2 d kT}\left[B\sigma^2 c - \frac{\gamma}{\delta_b} + \sigma l\right]$$

Ω = molecular vol.

D_b = grain boundary diffusion

δ = grain boundary width

l = crack tip radius

d = ½ grain diameter

γ = specific grain boundary surface energy

σ = applied stress

c = ½ crack length

$B = \pi(1-\nu^2)/2E$ (ν = Poisson's ratio; E = Young's modulus)

ACTIVATION ENTHALPY VALUES FOR SUBCRITICAL CRACKING IN GEOLOGICAL MATERIALS

	ΔT (°c)	ΔH (kJ.mole^{-1})	
QUARTZ			
a plane ⊥ z	20 – 200	67	} air H_2O vap. press. 0.1–0.5 Pa
	200 – 300	99	
	20 – 100	65	} H_2O vap. 300 Pa
	100 – 200	73	
	20 – 80	52.5	H_2O liq
5° to [oTio]	90 – 240	108	} H_2O vap.
	20 – 250	63	H_2O vap.
<c>	20 – 50	46 – 100	H_2O vap.
QUARTZITE	20 – 80	70	H_2O liq.
BASIC ROCKS	20 – 75	30 – 46	H_2O liq
CALCITE ROCKS	20 – 85	63 – 147	H_2O liq.
GRANITIC ROCKS	20 – 300	ca. 80 – 100	H_2O vap

Dn creep/glide ΔH. 163 Diffusion ΔH = 80–180, 130–220 paton

REACTION RATE THEORY OF CRACK GROWTH

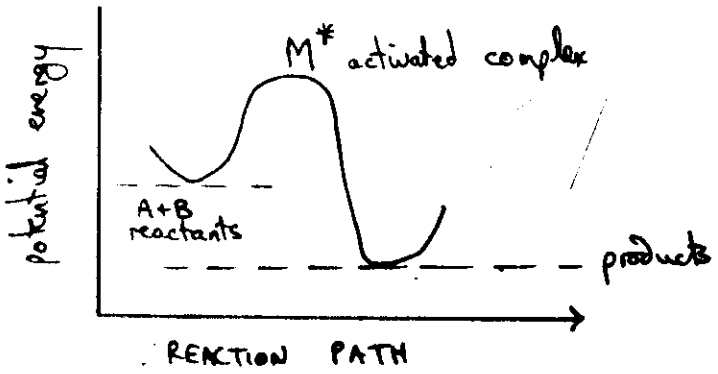

$$A + B \leftrightarrow M^* \rightarrow \text{products}$$

η = N° environmental species A reacting with a single each Sip bond B to give activated (weakened) state of bond (M^*).

$$H-O-H + [\equiv Si-O-Si\equiv] \leftrightarrow M^* \rightarrow 2[\equiv Si-OH]$$

Weakened state assumed to be

$$\equiv Si-OH \cdot HO-Si\equiv$$

Order of reaction

$$-dc/dt = kc^n$$

decrease in concentration (rate of transformation) $= -dc/dt$
untransformed concentration of reactant $= c$
n = exponent or ORDER
k = rate constant

INFLUENCE OF PRESSURE

For surface cracks or blunt internal cracks

1. If pore fluid has access to crack tips, and

$P_f = P_t$ ie $P_e = 0$

$$K_I = Y(\pi c)^{\frac{1}{2}} \sigma$$

σ ← applied remote macroscopic tensile stress

2. If pore fluid has access to crack tips but $P_f < P_t$ ie $P_e > 0$

$$K_I = Y(\pi c)^{\frac{1}{2}} (\sigma - P_e)$$

INFLUENCE OF ACTIVITY OF STRESS CORROSION AGENT

1. $a[H_2O]$ increases with P_f, T and depth in crust

2. $H_2O \leftrightarrow H^+ + OH^-$

K_w (ion product) $= a_{OH^-} \cdot a_{H^+}$

$a[OH^-]$ increases with P_f and depth ($\lambda \simeq 1$) but with T goes up (250°C) then does

3. $NaCl + H_2O \leftrightarrow NaOH + HCl$

∴ in high-temperature environments expect neutral or acid conditions to be rare.

SUMMARY OF SUBCRITICAL CRACK GROWTH DATA

1. Slopes of curves in $K - v$ space steep but highly variable.

   $v \propto K_I^n$

   $n = 12 \rightarrow 100$!

   Generally, the more microstructurally complex the material, the greater is the n value.

Physically, this means the greater the n value the smaller is the extent of subcritical crack growth
i.e the less important it is for geophysical problems.

2. Activation enthalpies generally low (50–100 kJ.mol) lower than for most intracrystalline plastic deformation processes.
But hard to associate with any particular mechanism.

WHAT DO WE KNOW ABOUT SUBCRITICAL CRACKING IN QUARTZ ROCKS? AND OTHER SILICATES?

1. Stress intensity factor dependence of crack velocity is high
This means can't easily distinguish between theoretical models by lab. expts.
2. Activation enthalpy depends on models + is hard to measure but is generally low.
3. Crack velocities down to ca. 10^{-11} m·s^{-1} measured experimentally.
4. Ranking of stress corrosion susceptibility ($\uparrow$ higher for microstructurally more complex rocks)
5. Crack velocity dependence on water pressure, activity suggests order of reaction involved in subcritical cracking is = 1.
6. Increasing concentration of OH^- ions increases the rate of crack propagation
7. Increasing temperature up to 300°C increases rate of crack growth.
8. Influence of pressure?
9. Region 2 and 3 probably restricted to small range of K values.
10. n depends on $p(H_2O)$. For [illegible]

PHYSICO-CHEMICAL BASIS OF STRESS CORROSION (SUBCRITICAL CRACKING)

[redacted]

1. [redacted] Rocks rarely consist of just quartz, however. Multiphase — other silicates → feldspar, mica, pyroxene/amphibole, olivine

   ← DO WEAKENING REACTIONS APPLY TO THESE MINERALS?

2. [redacted] As crack velocity decreases — crack path tends to become predominantly intergranular.

   ∴ What controls "stress corrosion" at slower velocities will be details of grain boundary surface chemistry and reaction of g.b.'s/matrix with agent.

   ? ? ?

CONCLUDE: DON'T KNOW WHAT IS MEANT BY 'STRESS CORROSION/SUBCRITICAL CRACKING' AT THE MICROMECHANICAL LEVEL — WHICH IS CRUCIAL FOR GEOPHYSICAL EXTRAPOLATION.

SUBCRITICAL CRACKING OF ROCKS

SUBCRITICAL CRACK GROWTH LIMIT

From Charles-Hilley

$$v = v_0 \exp\left[\alpha\sigma^* + \beta\sigma^{*2} - (\gamma/r_c)\right]$$

stress conc. | strain energy | interfacial en terms

A: High-order stress terms negligible

$$K_0 = \left[(QV_m)/2br_c\right] + \left[(RT)/b\right] \ln(c/2)$$

b given by $v = v_0 \exp(bK_I/RT)$

B: Strain energy term dominant

$$K_0 = \left[(Q E \pi/2) + (ERT/V_m)(\pi r_c) \ln(c/2)\right]^{1/2}$$

Q = interfacial energy

INFLUENCE OF STRESS ON HEALING RATES

Effect through chemical potential at crack tips

$$\mu_a = \frac{\gamma \Omega}{\ell}$$ in absence of stress

γ = specific surface energy
Ω = atomic volume
ℓ = crack tip radius

$$\mu_a = \frac{\Omega}{\ell}\left(B\sigma^2 c - \gamma\right)$$ when stressed

$B = \pi(1-\nu^2)/2E$
c = crack length

(1) Because stress enters as σ^2 for long thin cracks both tensile and compressive stress will reduce the driving force for crack spheroidization and sintering.

For small circular cracks compressive stress can inhibit sintering.

(2) For cracks length a where $a_c < a < a'_c$
(a_c ← growth limit; a'_c ← catastrophic growth)

lengthening by mass transport under tensile or compressive stress will occur.

Tensile stress → catastrophic failure
Compressive stress → only growth till stress forces crack [illegible]

CRACK HEALING

For grain boundary diffusion controlled

$$-dc/dt = \left[D_g w/4 r_c d\right]\left[1 - \exp(\mu_a N/RT)\right]$$

$$\mu_a = \gamma_b V_a / r_c$$

↑ chemical potential of atoms at crack tip

If crack stressed

$$\mu_a = (V_a/r_c)\left[B\sigma^2 c - \gamma_b\right]$$

Table 9. Subcritical crack growth limits for quartz

Mechanism	Temperature (°C)	Mode I stress intensity factor at growth limit ($MPa.m^{1/2}$)
Stress corrosion		
Case A	20	0.2
	200	0.19
Case B	20	0.39
	200	0.46
Grain boundary diffusion		
Case A	20	0.39
	200	0.22
Case B	20	0.38
	200	0.38

Note: K_{Ic} for quartz is approximately 1 $MPa.m^{1/2}$.

"Average" crack velocity of 10^{-12} $m.s^{-1}$ gives ≃ 1 cm of crack growth in 300 years (the recurrence time of some big quakes

"Average" crack velocity of 10^{-9} $m.s^{-1}$ gives 3 cm/year

Although slow these velocities are geophysically significant.

WHAT HAPPENS TO {SUBCRITICAL CRACKING / STRESS CORROSION} PROCESS IN GEOLOGICAL ENVIRONMENTS?

A. Will depend on detailed nature of process.

B. From what we know of variation of T, P_T, P_f and a [agent] with crustal depth — can construct possible patterns of behaviour.

B1. If molecular water is the agent.

a $[H_2O]$ increases with increase in P_f, T and depth

∴ Should get an increase in crack growth rates with ~~in~~ depth.

But fugacity $[H_2O]$ changes by only about 1½ orders throughout the crust.

B2. If ionized water or hydroxyl involved

$$H_2O \leftrightarrow H^+ + OH^-$$

$$K_w = a_{OH^-} \cdot a_{H^+}$$

$K_w = 10^{-14}$ @ R.T.
$= 10^{-8}$ at base of crust

a $[OH^-]$ increases with water pressure, increases with depth (if $\lambda = 1$) but after slight increase will decrease with temperature.

Substantial changes possible in this variable.

[Is this a way of distinguishing between 2 potential agents?]

B3. Because water becomes a stronger acid than most common ones at depth — it will displace them from their salts

e.g. $NaCl + H_2O \leftrightarrow NaOH + HCl$

These neutral or acid conditions should be rare in high-temperature environments

LEVELS OF SHEAR STRESS IN FAULT ZONES

Problem: Current estimates vary by at least 1 order of magnitude Hence major problems such as

- driving mechanism of plate tectonics
- energetics of crustal faulting

are entirely unresolved.

Deviatoric

1. [redacted] stress can only be measured directly very close to the earth's surface
   by overcoring
   hydrofracturing
   wire stress meters
   } etc

2. It becomes necessary to infer from secondary lines of evidence what the level of shear + other stresses might be.

Generally: 2 schools of thought

① Shear stress is "high" $\geq$ 1,000 bars

② Shear stress is "low" $\simeq$ 100 bars

STRESS LEVELS IN FAULT ZONES; SOME

INDIRECT LINES OF EVIDENCE

1. Laboratory studies of rock friction
2. Seismology
3. Heat-flow anomalies around fault zones
4. Geological evidence → fault rock textures
   → hydrothermal veining, etc.
5. Microstructural paleopiezometers
6. Laboratory studies of stress memory effects.

DIRECT LINES OF EVIDENCE

1. Hydrofracturing
2. Overcoring - stress relief
3. Wire stress meters (really strain meters) } surface or near-surface

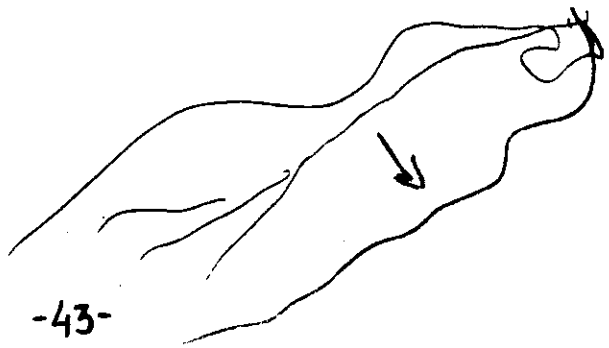

Empirical relations have been established in metals between the dislocation microstructures and deviatoric stress and their applications in the case of rocks discussed by Nicolas & Poirier (1976, p. 137). The main relations tie the dislocation curvature, the dislocation density and the subgrain size to the applied stress.

Durham, Goetze & Blake (1977) have considered the relation between the minimum radius of curvature (R, measured in micrometres) of dislocation loops and the stress (σ, measured in kilobars) in olivine. They observe a fairly good experimental correlation:

$$\sigma \approx 0.6 R^{-1},$$

which when compared with the expected relation

$$\sigma = K \mu b R^{-1},$$

where μ is the shear modulus and b the Burgers vector, yields a K value of 1.84×10^{-6} kbar cm.

The relation between the free dislocation density (ρ) and the stress has been experimentally investigated by Kohlstedt & Goetze (1974), by Goetze (1975*a*, *b*) and by Durham *et al.* (1977) who find a good experimental correlation expressed in the general form:

$$\sigma = K' \mu b \rho^{\frac{1}{2}},$$

$$\sigma = 9 \times 10^{-4} \rho^{0.5} \text{ (Goetze 1975}a, b\text{)},$$

$$\sigma \approx 2 \times 10^{-3} \rho^{0.53} \text{ (Durham } et\ al.\text{ 1977)}.$$

The relation between the subgrain size (d, measured in micrometres) and the maximum stress is expected to have the following form:

$$\sigma = K'' \mu b d^{-1}.$$

In olivine, the [100] tilt wall spacing is principally measured, due to its predominance over any other substructure and to its smallest spacing when compared to the other subboundary systems. The considered subgrains are only those optically visible and not those which subdivide them at the t.e.m. scale (Green & Radcliffe 1972). They are now observed using a new decoration technique (Kohlstedt, Goetze, Durham & Vander Sande 1976) which, making it possible to observe about ten times as many tilt walls than before, can explain the large discrepancy between Raleigh & Kirby's (1970), Goetze's (1975*a*, *b*), Mercier's (1976) and Durham *et al.* (1977) relations.

$$\sigma = 17 d^{-1} \quad \text{(Geotze 1975}a, b\text{)},$$

$$\sigma = 118 d^{-1} \quad \text{(Mercier 1976)},$$

$$\sigma = 10 d^{-1} \quad \text{(Durham } et\ al.\text{ 1977)}.$$

The size of dynamically recrystallized olivine grains (neoblasts) has also been considered as a potential geopiezometer for mantle rocks. The following experimental relations have been found:

$$\sigma = 11 d^{-0.5} \quad \text{(Goetze 1975}a, b\text{)},$$

$$\sigma = 19 d^{-0.67} \quad \text{(Post 1973)},$$

$$\sigma = 60 d^{-0.83} \quad \text{(Mercier 1976)}.$$

Mercier obtains a weak temperature dependence for this relation:

$$d = 1.12 \sigma^{-1.4} \exp(13500/RT).$$

Otherwise, as expected from the metallurgical literature, no temperature dependence is found for all these relations.

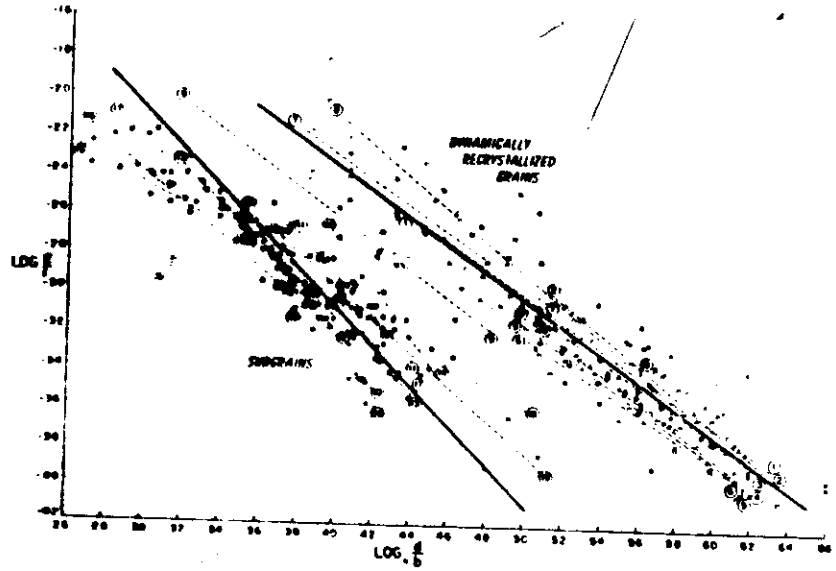

Figure 1

Non-dimensional plot of experimentally determined stress vs. subgrain size and recrystallized grain size for steady state creep. The key to the symbols is in Table 1. Data were rendered non-dimensional by constants in Table 2. Dashed lines are unweighted linear regressions to individual data sets. Each solid line is a best fit to the respective group of data for subgrains and recrystallized grains. The slope of the solid line is taken to be the mean of the slopes of the data sets in each group. The theoretical equation fits the solid lines equally for physically reasonable values of the empirical parameters.

MAXIMUM FRICTION

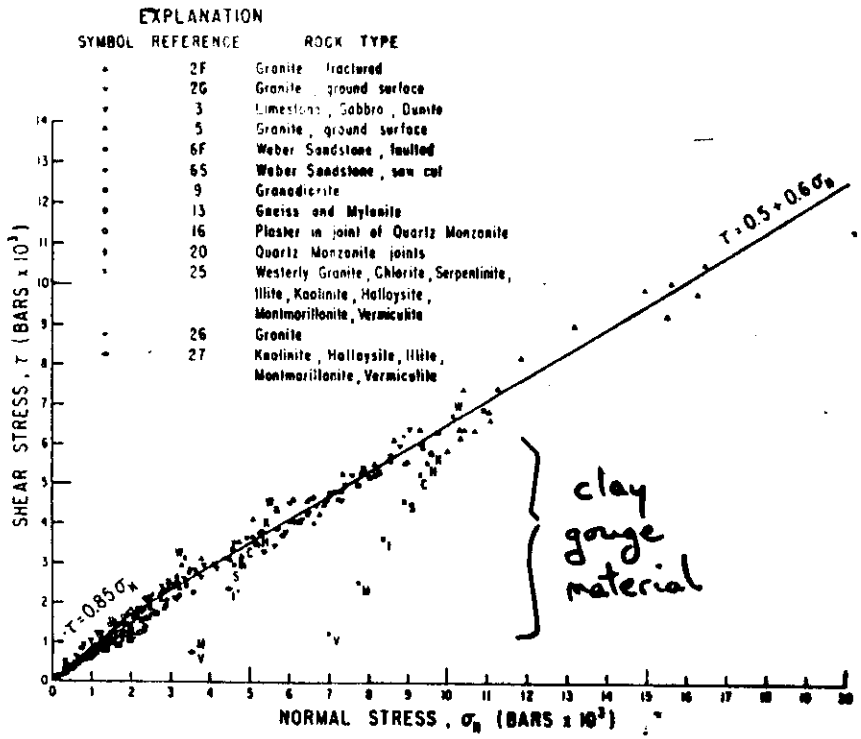

Figure 7

Shear stress plotted as a function of normal stress at the maximum friction for a variety of rock types at normal stresses to 20 kb.

Clay minerals not likely to be stable below ≲ 10 km.

EFFECT OF TEMPERATURE ON SLIDING STRESS OF WESTERLY GRANITE

(Saw cuts)

$$\tau = 0.5 + 0.6\,\sigma_n$$

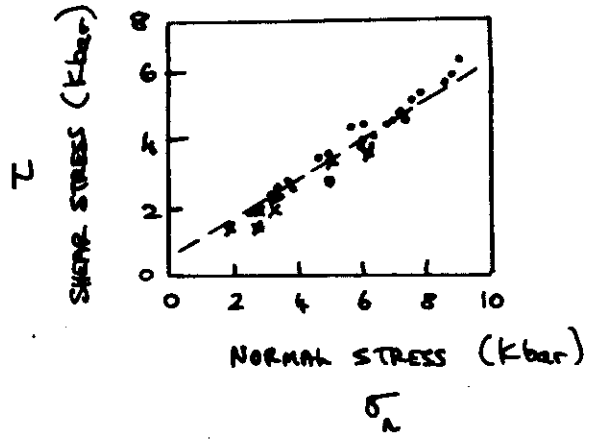

- • 20°C
- x 100°C
- x 300°C
- • 400°C
- x 500°C

LABORATORY STUDIES OF ROCK FRICTION

1. Byerlee's law:

For sliding to occur

$$\tau_f = \mu(\sigma_n - P_f)$$

μ = coeff. of static friction

μ is largely independent of rock type.

2. To get low shear stress requires pore fluid pressures $\simeq$ lithostatic. From $\bar{\sigma}_{ij} = \sigma_{ij} - P_{fluid}\,\delta_{ij}$ – effective stress law. This may occur transiently in earthquake faulting – but permeability data for crust (Brace) suggest that will not be a general condition for earthquake fault zones. Transient increase in P_f due to shear heating – expansion of water in pore space.

Pore fluid pressures are likely to exceed hydrostatic if impermeable cap rocks present. Pore fluids, if not present everywhere, are at least very common in the upper crust.

THUS: LAB DATA SUGGESTS SHEAR STRESSES $\geq$ 1kb or more UNLESS $P_f \simeq P_{load}$

...GICAL EVIDENCE

1. Stress drops for most earthquakes are low $\simeq$ 100 bars or so for the large ones. Although exceptions where stress drop is high do occur.

2. Can this be taken to mean that the average ambient shear stress is $\simeq$ 100 bars also?

3. If pore water is present then provided shear strain > 1 near-total stress drops must occur because of seismogenic shear heating of pore water increasing pore water pressure and decreasing effective normal stress on fault to near zero. $(\sigma_{eff} = \sigma_t - p)$

4. Only requirement is that hydraulic diffusivity of fault rock is lower than thermal diffusivity so that fluid flow away from fault does not take heat away.

Estimated values for S.A.F. (1 kb, 300°C)

hydraulic diffusivity = $10^{-4} - 10^{-5}$ cm^2 s^{-1}

thermal diffusivity = 10^{-2} cm^2 s^{-1}

MAXIMUM INCREASE IN PRESSURE OF WATER IN FAULT DUE TO SEISMOGENIC HEATING AT SLIP VELOCITIES OF METRES/SEC

Average Shear Stress (bars) $\bar{\tau}$	Displacement (cm) u	Width (cm) $2a$	Shear Strain γ	time (s)	Permeability (cm^2)	Pore pressure increase (bars) ΔP
50	10	2	5	0·1	10^{-14}	150
50	10	10	1	0·1	2×10^{-13}	30
50	100	2	50	1·0	10^{-15}	1,500
50	100	10	10	1·0	2×10^{-14}	300
500	10	2	5	0·1	10^{-14}	1,500
500	10	10	1	0·1	2×10^{-13}	300
500	100	2	50	1·0	10^{-15}	15,000
500	100	10	10	1·0	2×10^{-14}	3,000
500	100	100	1	1·0	2×10^{-13}	300

From $\frac{dp}{d\bar{\tau}} = 0.6\,\gamma$ $\quad \left[\gamma = \frac{u}{2a}\right]$

$\frac{dp}{d\bar{\tau}}$: change in pressure with shear stress

γ: shear strain

HEAT FLOW ANOMALIES

Steady aseismic shearing across fault zone with shear resistance τ_f gives a constant heat flow per unit volume of the zone

$$\dot{H} = (\tau_f \cdot v)/w$$

v = slip rate , w = width of zone

If shear stress high enough over long enough period — can get shear heating leading to heat flow anomalies.

e.g. 1C m wide shear zone, displacement of 1 km at 1→10 cm/yr against shear resistances of 100 bars → 1 kbar.

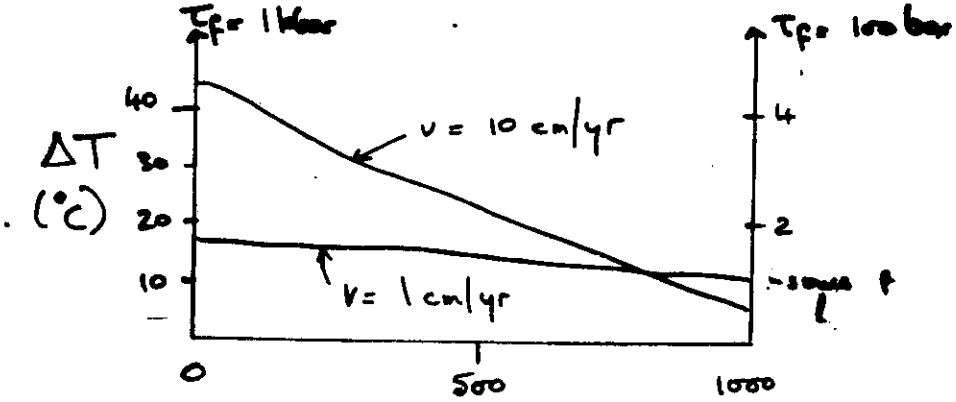

NB: 1. Rise in temperature occurs over a much broader region than fault (10 m wide in this case).

2. Steepness of thermal gradient increases with slip rate

3. High shear stress is required to generate heat anomaly

ABSENCE OF HEAT FLOW ANOMALY OVER SAN ANDREAS FAULT

1. Over segment of S.A.F. that is not creeping and which produced a great earthquake in 1857 no measurable perturbation of the regional value of 1.6 heat flow units occurs.

This is consistent with a low ambient shear stress of ≲ 150 bars maximum.

∴ [UNLESS]

Heat generated is dissipated by convective circulation of water, which

Would require a thermal spring flowing at 10,000 litres/hr at 100°C

At every kilometre along fault.

This is not observed —

SAF shows absence of thermal springs except in Imperial Valley where volcanic heat sources exist.

If convection pushes heat away from fault this would get high heat flow over broad region not peak over fault.

This is not observed either.

energy dissipated by other means

e.g. phase change (dehydration or melting)

Creation of new surface area by comminution

Neither of these can absorb enough energy to explain away a shear heating anomaly.

GEOLOGICAL EVIDENCE: HYDROTHERMAL VEINING, etc.

1. Many faults show en-echelon mineralized hydrofractures and other sorts of hydrothermal veining.
Spatial and textural arrangement suggests they formed at same time as fault.

Condition for their formation is that

$$P_{fluid} > \sigma_{3\,(overburden)}$$

by an amount = tensile strength of rock

∴ Implies high pore fluid pressures.

2. Other fault zones show no such evidence
∴ perhaps "dry".

Remember exhumed fault zones seen at surface represent past state at depth.

Type 1 fault zones (ie wet) are seem most common.

& No hydrothermal veining in Alpine Fault
& Hydrothermal veining in San Andreas Fault

IMPLICATIONS OF PRESENCE OF PSEUDO-TACHYLYTE ON FAULTS

1. Field evidence suggests that generation & injection of pseudo-tach. melt took place within a few seconds — implying 'seismic' slip rate of $\sim 10\,cm\,s^{-1}$

2. Melting on fault planes is inhibited by presence of pore fluids.
Because frictional heating creates on a transient localized increase in fluid pressure (from P, V, T data for water) that drastically lowers the effective normal stress across the fault plane, and thus the capacity of the fault to generate heat by further slip.
Thus pseudotachylyte a product of dry faulting.

3. Because rocks are dry and from τ_f / slip displacement graph - high shear stress of ~ kilobars is required to initiate pseudotachylyte generation

4. As frictional resistance drops with displacement - Once fault is 'lubricated' by presence of melt then would expect almost total stress relief — and possibly large earthquakes.

IMPLICATIONS OF PRESENCE OF PSEUDO TACHYLYTE ON FAULTS

Field observations show that displacement (d) on pseudotachylyte faults is related to thickness (a) of melt rock by

$$d = K a^2 \qquad K \leq 500$$

Heat generated per unit area of fault after displacement d $\propto$ thickness of melt layer

$$H = \int_{x=0}^{x=d} \tau_f \cdot dx = 2\sqrt{(d/K)}$$

τ_f = frictional resistance, Q = heat to melt unit volume of rock.

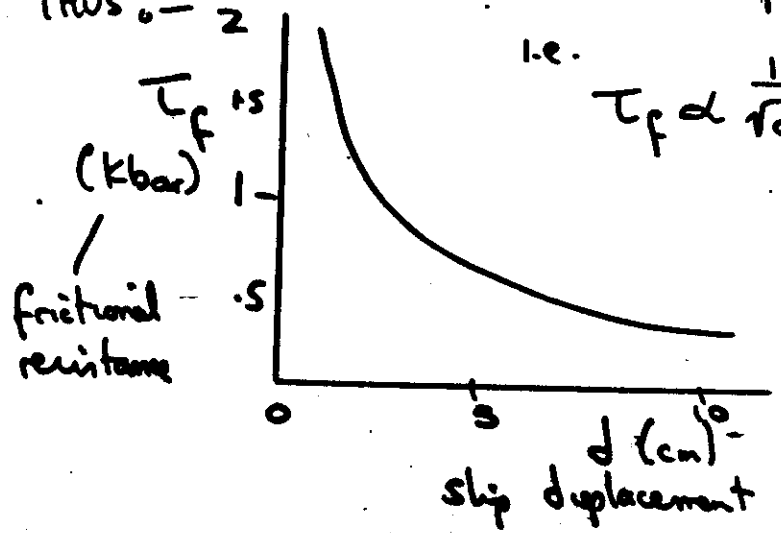

i.e. $\tau_f \propto \frac{1}{\sqrt{d}} \propto \frac{1}{a}$

Frictional resistance falls off with displacement

MECHANICAL TWINNING IN MINERALS AS A STRESS INDICATOR

Advantages: Occurs under critical resolved shear stress that is independent of temperature and strain rate and does not appear to be affected by σ_3 or pore fluid pressure.

Most useful: Calcite, dolomite, Clinopyroxene

	Calcite	Dolomite	Clinopyroxene
Critical shear stresses for twinning on key systems $\simeq$	100 bars	1000 bars	1400 bars

N.B. Shear stress supported by aggregate varies because not all grains favourably oriented for twinning and some intracrystalline slip must also occur to satisfy Von Mises ductility criterion (5 independent slip systems)

Reduction in shear stress supported by aggregate with T increase or $\dot{e}$ decrease due to fact that T and $\dot{e}$ - dependent intracrystalline slip is also occurring.

FROM DEFORMATION MICROSTRUCTURES

Recrystallized grain size: $(\sigma_1-\sigma_3) = A \cdot D^{-m}$

($\sigma_1-\sigma_3$: diff. stress; D: grain size; A, m are constants)

e.g. Quartzite

$(\sigma_1-\sigma_3) = 381 \cdot D^{-0.71}$

[MPa] [microns]

Dislocation density: $(\sigma_1-\sigma_3) = \alpha \mu b N^{0.5}$

(μ: shear modulus (GPa); b: Burgers vector (nm); N: dislocation density)

e.g. Quartz

$N = 1.6 \times 10^4 (\sigma_1-\sigma_3)^{1.5}$

MPa

e.g. Coyote Mtn Mylonite

Problem: ① Very sensitive to environmental parameters
② Based on little experimental data
③ Affected by post deformation annealing

LAB STUDIES OF STRESS MEMORY EFFECTS

Kaiser effect: Rock subject to cyclic loading only exhibits significant acoustic emission when stressed in the second and subsequent cycles after the maximum stress in previous cycles has been exceeded.

e.g.

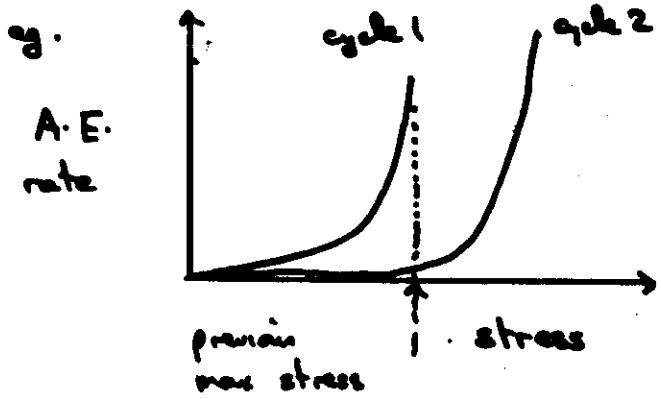

Mogi found sometimes not clear in simple experiments so suggested that the DIFFERENCE in AE activity between cycles is used as an indicator of previous max. stress. This increases markedly once the previous max stress exceeded.

Problems: - ① What about annealing / recrystallization through creep and memory loss

② Kaiser effect not seen in cases of dilatancy embrittlement where fracture stress.

STRESS LEVELS IN VICINITY OF SAN ANDREAS FAULT FROM HYDROFRACTURE DATA

Zoback et al.

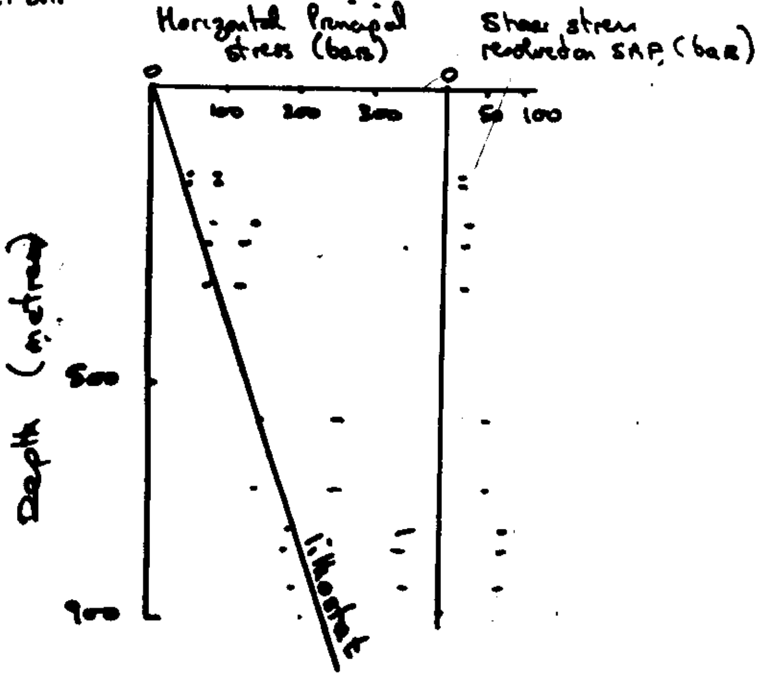

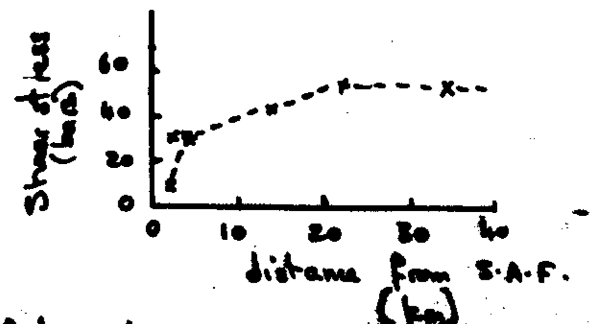

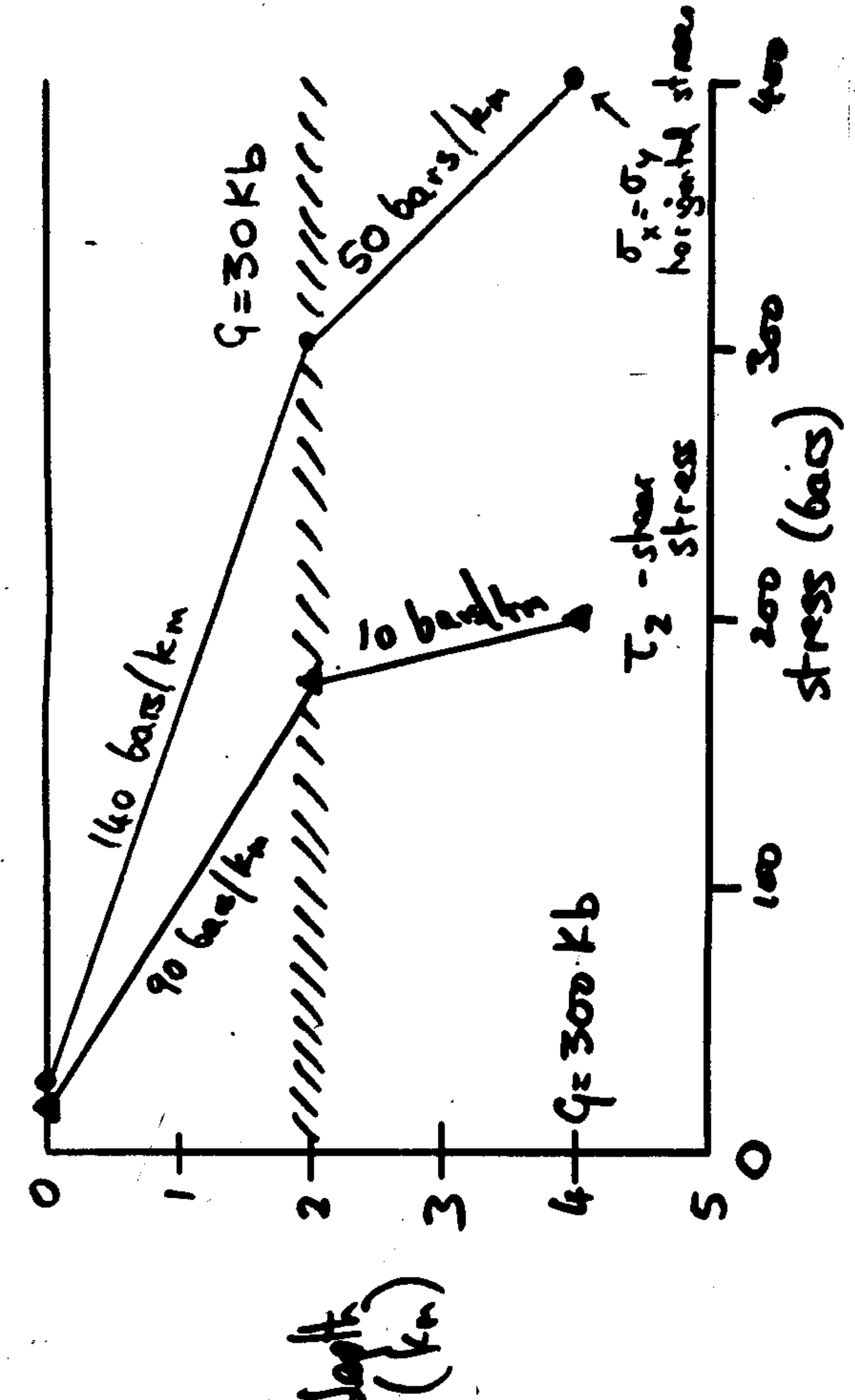

Extrapolation to seismogenic depths on SAF suggests
shear stress of several hundred bars — but no increase to
step-like Zoback thinks it is near surface effect and
extrapolation not justified. But note [illegible]

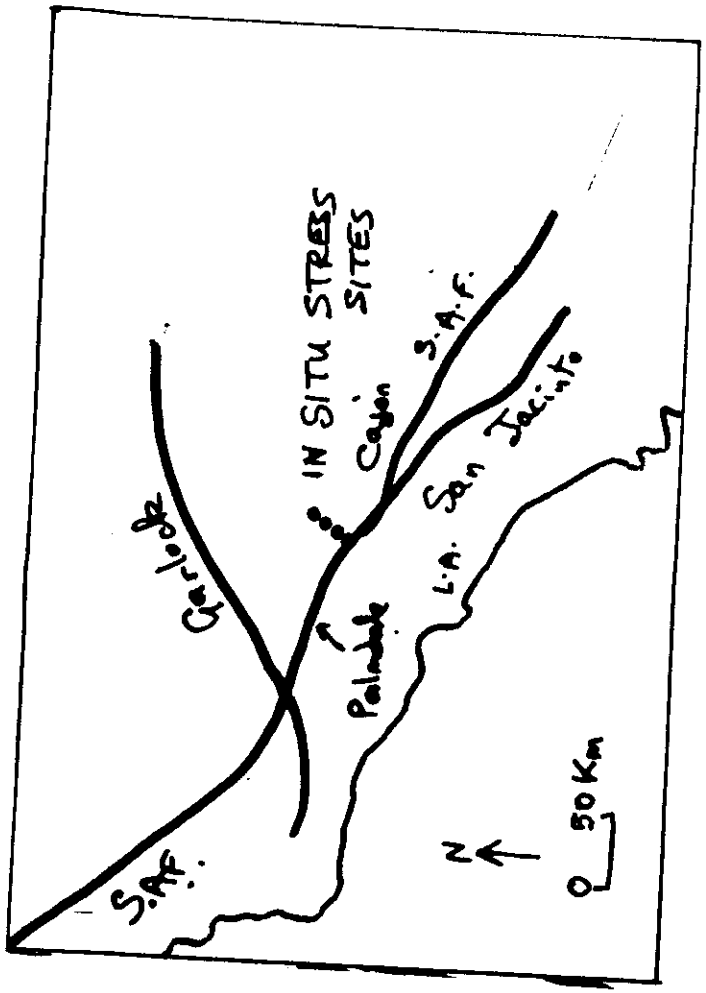

IN-SITU STRESS

1. Vertical stress gradients are proportional to horizontal gradients of vertical surface deformation.

2. Actual displacement measurements around San Andreas Fault are consistent with a layered crust — not simple model usual used to interpret in-situ stress measurements.

3. Over tectonic time-scale crust has vertically increasing rigidity. Modelled in figure.

4. In-situ hydrofracturing measurements are very shallow and don't top deeper trends.

5. Actual shear stress gradient at depth is more likely to be
   ~ 10 bars/km

6. Over seismogenic zone — leads to average shear stress of
   ≤ 225 bars

ALPINE FAULT	SAN ANDREAS FAULT
SHEAR HEATING	NO SHEAR HEATING
1. METAMORPHIC ISOGRADS ARE PARALLEL TO FAULT AND STEEP TO VERTICAL. DECREASING IN GRADE AWAY FROM FAULT	NO OBVIOUS LINK BETWEEN METAMORPHISM AND FAULT AS IT IS AT PRESENT
2. HORIZONTAL TEMPERATURE GRADIENT OF 40°C/km INDICATED FROM ISOGRADS.	
3. SHEAR STRESS < 1 kbar CANNOT PRODUCE THIS HEAT UNLESS SLIP VELOCITIES BETWEEN PLATES ARE > 10 cm/yr.	SHEAR STRESS OF CA. 100 bars IS CONSISTENT WITH HEAT FLOW DATA.
4. SOLUTES UP TO 15 km AWAY FROM FAULT ARE DEPLETED IN RADIOGENIC ARGON THAT CANNOT BE EXPLAINED BY SIMPLE UPLIFT.	
5. POSSIBLE HEAT FLOW ANOMALY	NO HEAT FLOW ANOMALY NOT ENOUGH THERMAL SPRINGS NOT ENOUGH COMMINUTION OR DEHYDRATION
6. SHEAR STRESS (long term) [redacted]	SHEAR STRESS (long term) [redacted]

[redacted]

SUMMARY

1. Some faults 'wet', some 'dry'
   ie have high or low pore fluid pressure
   'Wet' are more common
2. Dry faults may support high shear stress ~ 1000 bars
   Wet faults may only support low shear ~ 100 bars
   during seismic and aseismic shearing.

But what is mechanism?

Although transient pore pressure rise in earthquake faulting due to shear heating may drop effective normal stress on fault
This cannot work for aseismic shearing as pressure dissipated over longer time available.

* Pore fluid pressures are generally not → lithostatic
but where present may be → hydrostatic.
Lab. expts to date have shown high frictional resistance under these conditions.

Resolution & dilemma & [redacted]
in recent expts.

→ unless argillaceous cap rocks prevent healing

[redacted]